NeuroImage 202 (2019) 116070

Contents lists available at ScienceDirect

NeuroImage

journal homepage: www.elsevier.com/locate/neuroimage

Transdiagnostic variations in impulsivity and compulsivity in obsessive-compulsive disorder and gambling disorder correlate with effective connectivity in cortical-striatal-thalamic-cortical circuits

Linden Parkes [a,*], Jeggan Tiego [a], Kevin Aquino [a], Leah Braganza [a,b], Samuel R. Chamberlain [c], Leonardo F. Fontenelle [a,d], Ben J. Harrison [b], Valentina Lorenzetti [a,e], Bryan Paton [f,g], Adeel Razi [a,h,i], Alex Fornito [a,1], Murat Yücel [a,1]

[a] The Turner Institute for Brain and Mental Health, School of Psychological Sciences, and Monash Biomedical Imaging, Monash University, Victoria, Australia
[b] Melbourne Neuropsychiatry Centre, Department of Psychiatry, The University of Melbourne and Melbourne Health, Victoria, Australia
[c] Department of Psychiatry, University of Cambridge and Cambridge Peterborough NHS Foundation Trust, Cambridge, United Kingdom
[d] Obsessive, Compulsive, and Anxiety Spectrum Research Program, Institute of Psychiatry, Federal University of Rio de Janeiro & D'Or Institute for Research and Education, Rio de Janeiro, Brazil
[e] School of Psychology, Faculty of Health, Australian Catholic University, Fitzroy, Australia
[f] School of Psychology, Faculty of Science, University of Newcastle, Newcastle, Australia
[g] Cognition & Philosophy Lab, Monash University, Melbourne, Australia
[h] Wellcome Centre for Human Neuroimaging, Institute of Neurology, University College London, United Kingdom
[i] Department of Electronic Engineering, NED University of Engineering and Technology, Karachi, Pakistan

ARTICLE INFO

Keywords:
Impulsivity
Compulsivity
Disinhibition
OCD
GD
DCM

ABSTRACT

Individual differences in impulsivity and compulsivity is thought to underlie vulnerability to a broad range of disorders and are closely tied to cortical-striatal-thalamic-cortical function. However, whether impulsivity and compulsivity in clinical disorders is continuous with the healthy population and explains cortical-striatal-thalamic-cortical dysfunction across different disorders remains unclear. Here, we characterized the relationship between cortical-striatal-thalamic-cortical effective connectivity, estimated using dynamic causal modelling of resting-state functional magnetic resonance imaging data, and dimensional phenotypes of impulsivity and compulsivity in two symptomatically distinct but phenotypically related disorders, obsessive-compulsive disorder and gambling disorder. 487 online participants provided data for modelling of dimensional phenotypes. These data were combined with 34 obsessive-compulsive disorder patients, 22 gambling disorder patients, and 39 healthy controls, who underwent functional magnetic resonance imaging. Three core dimensions were identified: disinhibition, impulsivity, and compulsivity. Patients' scores on these dimensions were continuously distributed with the healthy participants, supporting a continuum model of psychopathology. Across all participants, higher disinhibition correlated with lower bottom-up connectivity in the dorsal circuit and greater bottom-up connectivity in the ventral circuit, and higher compulsivity correlated with lower bottom-up connectivity in the dorsal circuit. In patients, higher clinical severity was also linked to lower bottom-up connectivity in the dorsal circuit, but these findings were independent of phenotypic variation, demonstrating convergence towards behaviourally and clinically relevant changes in brain dynamics. Effective connectivity did not differ as a function of traditional diagnostic labels and only weak associations were observed for functional connectivity measures. Together, our results demonstrate that cortical-striatal-thalamic-cortical dysfunction across obsessive-compulsive disorder and gambling disorder may be better characterized by dimensional phenotypes than diagnostic comparisons, supporting investigation of quantitative liability phenotypes.

* Corresponding author. 770 Blackburn Road, Clayton, Victoria, 3168, Australia.
E-mail address: lindenmp@seas.upenn.edu (L. Parkes).
[1] These authors contributed equally.

https://doi.org/10.1016/j.neuroimage.2019.116070
Received 8 March 2019; Received in revised form 24 July 2019; Accepted 2 August 2019
Available online 2 August 2019

1. Introduction

Psychiatric research is gradually shifting away from studying classically diagnosed disorders towards an understanding of the underlying constructs and mechanisms that drive maladaptive behavior (Cuthbert and Insel, 2013; Insel et al., 2010). In this context, impulsivity and compulsivity feature prominently as putative intermediate phenotypes linked to symptom variation across multiple disorders (Chamberlain et al., 2017; Dalley et al., 2011; Fineberg et al., 2014, 2010; Fontenelle et al., 2011), and likely explain a substantial fraction of commonly observed comorbidities (Chamberlain et al., 2017; Gillan, Kosinski, Whelan, Phelps and Daw, 2016a; Tiego et al., 2018). Impulsivity refers to acting without forethought or regard to potential adverse consequences. Compulsivity refers to a tendency toward repetitive behavioral patterns that are insensitive to outcomes and/or may be accompanied by undesirable consequences.

Historically, impulsivity and compulsivity have been quantified using scores on either behavioral tasks (e.g., response inhibition paradigms) or self-report questionnaires (Cyders and Coskunpinar, 2011; Robbins et al., 2012), although the relation between the two constructs has been unclear (Dalley et al., 2011; Fineberg et al., 2014); some suggest that they are diametrically opposed on a single continuum (Hollander, 1993; Hollander and Benzaquen, 1997), whereas others propose that they are orthogonal dimensions (Fineberg et al., 2010; Fontenelle et al., 2011). Recent Confirmatory Factor Analyses (CFA) of multiple measures of impulsivity and compulsivity has shown that the constructs form two distinct but positively correlated traits, which each predict poorer quality of life (Chamberlain et al., 2017). Using Structural Equation Modelling (SEM) of self-report data acquired from a large normative sample, we characterized a bifactor model in which a unitary, general 'disinhibition' dimension, characterized by high impulsivity, uncertainty intolerance and obsessive beliefs, coupled with low desire for predictability, perfectionism, and threat estimation, was the strongest predictor of the co-occurrence of addictive and obsessive-compulsive symptomatology, with residual, specific dimensions of 'impulsivity' and 'compulsivity' explaining additional unique variance (Tiego et al., 2018). Thus, our model successfully captures both correlated (disinhibition) and orthogonal variance associated with different measures of impulsivity and compulsivity that are relevant to understanding behavior and psychopathology.

One implication of our model is that clinically diagnosable disorders of impulsivity and compulsivity represent extreme expressions of traits that are distributed continuously with the healthy population (the continuity hypothesis). This postulate, while consistent with the implicit assumption of the Research Domain Criteria (RDoC) initiative (Cuthbert and Insel, 2013; Insel et al., 2010), has seldom been formally tested in psychiatry. Hence, it remains unclear how subclinical variation in impulsivity and compulsivity relate to case-level psychopathology, either at the level of observable behavior or underlying neurobiology.

Here, we test the continuity hypothesis using impulsivity and compulsivity as intermediate phenotypes and diagnosed gambling disorder (GD) and obsessive-compulsive disorder (OCD) as exemplars of psychopathology at the extreme ends of these phenotypes. GD and OCD are both associated with dysfunctional levels of impulsivity and compulsivity (Grassi et al., 2015; Prochazkova et al., 2017; Tavares and Gentil, 2007; van Timmeren et al., 2018; Verdejo-García et al., 2008) and have overlapping pathophysiology centered on cortical-striatal-thalamic-cortical (CSTC) circuits (Harrison et al., 2013; Jung et al., 2016; Koehler et al., 2013; Peters et al., 2013), which are thought to play a critical role in mediating impulsive and compulsive behaviors (Everitt and Robbins, 2005, 2013; Everitt et al., 2008; Fineberg et al., 2014; Gillan, Robbins, Sahakian, van den Heuvel and van Wingen, 2016b). An advantage of studying a behavioral addiction such as GD is that it allows us to uncover pathophysiological processes without the confounding effects of substance abuse or dependence (Clark and Limbrick-Oldfield, 2013; Goudriaan, Oosterlaan, de Beurs, & van den Brink, 2004; Limbrick-Oldfield et al., 2013).

The CSTC circuitry of the brain comprises a series of parallel yet integrated loops that topographically connect distinct regions of frontal cortex predominantly with ipsilateral striatum and thalamus (Haber, 2003; Haber and Knutson, 2009). These circuits are functionally specialized and broadly segregate into ventral limbic, dorsal associative, and caudal sensorimotor systems (Anderson et al., 2018; Haber, 2003; Haber and Knutson, 2009; Parkes et al., 2017). Altered function of the dorsal and ventral circuits has been similarly implicated in both GD and OCD (Balodis et al., 2012; Choi et al., 2012; Figee et al., 2013; Gillan et al., 2015; Harrison et al., 2013, 2009; Koehler et al., 2013; Peters et al., 2013; Reuter et al., 2005; van Holst, Veltman, Büchel, van den Brink and Goudriaan, 2012b; Worhunsky et al., 2014).

Regarding OCD, recent meta-analytic work revealed that while CSTC dysconnectivity is consistently implicated in OCD, the direction (i.e., hypo- or hyper-connectivity with respect to healthy individuals) remains unclear (Gürsel et al., 2018). Recent work by Gillan et al. (2015, 2014; 2011) has suggested that CSTC dysfunction in OCD might be best understood in terms of a dysfunctional goal-directed system that causes an over-reliance on habitual/compulsive behaviours. Using a shock-avoidance task, participants were trained to press a lever to avoid an electric shock administered to the arm. After extensive training, the apparatus that delivered the shock was disconnected in full view of the participants, rendering the threat devalued (Gillan et al., 2014). Gillan et al. found that OCD patients continued to press the lever to avoid the shock despite the devalued threat. In a follow-up task-based fMRI study, OCD patients that developed avoidance habits after training showed positive functional connectivity between the dorsal striatum and the ACC whereas negative functional connectivity was observed between the same pair of regions in OCD patients who did not develop avoidance habits. Gillan et al.'s work demonstrates that the development of compulsions in OCD may be associated with dysfunctional habit formation, linked to changing dynamics in CSTC circuits. It remains unclear whether these findings generalise to the resting-state as well as other measures of compulsivity.

The neuroscience literature on GD is relatively sparse when compared to OCD. Nevertheless, evidence suggests that CSTC circuits are also central to the pathophysiology of GD (Balodis et al., 2012; Choi et al., 2012; Koehler et al., 2013; Peters et al., 2013; Reuter et al., 2005; van Holst, van Holstein, van den Brink, Veltman and Goudriaan, 2012a; van Holst et al., 2012b; Worhunsky et al., 2014). Some rs-fMRI studies have shown increased functional connectivity between PFC and ventral striatum in GD patients compared to HCs (Koehler et al., 2013). Task-based fMRI studies have shown increased functional connectivity between the ventral striatum and ACC relative to HCs while GD patients perform delay and probability discounting tasks (Peters et al., 2013) as well as go/no-go tasks (van Holst et al., 2012a). Finally, studies using reward/loss tasks, such as the monetary incentive delay task (MIDT), have found that, relative to HCs, GD patients show reduced activity in the ventral striatum and VMPFC during receipt of wins (Reuter et al., 2005) and the anticipation of wins and losses (Balodis et al., 2012), as well as increased activity in the dorsal striatum and OFC during probabilistic reward tasks (van Holst et al., 2012b). Together, these studies suggest that, like OCD, the pathophysiology of GD is characterized by dysfunction distributed across dorsal and ventral CSTC circuits.

Despite a common link to CSTC dysfunction, a direct comparison of GD and OCD is lacking in the literature. Such a comparison has the potential to uncover the degree to which any neural similarities or differences relate to variations in impulsivity and compulsivity. Some have suggested that the ventral and dorsal striatum respectively drive impulsive and compulsive behaviors, while cortical projections inhibit or regulate these behaviors (Fineberg et al., 2014), but these assertions have not been directly tested. Moreover, most work to date has relied on simple (undirected) models of network interactions, based on correlational measures of functional coupling between regions (i.e., functional connectivity), which cannot disentangle causal influences in CSTC circuitry.

In this study, we addressed two primary aims. First, we extended our prior modelling work (Tiego et al., 2018) by combining our existing normative cohort with a new sample of healthy controls (HCs), individuals with OCD, and individuals with GD to replicate our model and formally test the continuity hypothesis; that is, whether GD and OCD participants lie at the extreme ends of our quantitative phenotypes. Second, we investigated how the quantitative and clinical phenotypes relate to CSTC function. We mapped the effective connectivity (i.e., the causal interactions between brain regions) of the CSTC circuitry using Dynamic Causal Modelling (DCM) (Friston et al., 2003; Razi and Friston, 2016; Razi et al., 2017; Stephan et al., 2010) of resting-state functional Magnetic Resonance Imaging (rs-fMRI) data and linked effective connectivity parameters to our quantitative impulsivity and compulsivity phenotypes, as well as to traditional diagnostic groupings, in a Bayesian framework. As opposed to undirected estimates of functional connectivity, our approach allowed us to distinguish directional influences in CSTC circuitry, and to evaluate whether quantitative trait variation or diagnosis is a stronger correlate of brain function.

2. Methods and materials

2.1. Participants

Data were obtained from two independent samples. The first consisted of 487 participants (50.7% female) aged 18–55 years ($M = 34.2$, $SD = 9.3$) recruited online through the Amazon Mechanical Turk community, hereafter referred to as the '*online dataset*'. The online dataset consisted of individuals from the United States (93.3%), with a small proportion from Australia (6.1%). Participants provided written informed consent prior to completing an online battery of self-report questionnaires and were reimbursed $2 (USD) per hour for their time. In order to comprehensively model the full spectrum of impulsivity and compulsivity and not restrict analysis to the healthy range, participants in the online dataset were not excluded based on the presence of psychopathology. Data from the online dataset can be accessed at the Open Science Framework (https://osf.io/qa9eh/).

The second dataset consisted of 39 HCs, 34 patients with obsessive-compulsive disorder (OCD), and 23 patients with gambling disorder (GD) that were recruited as part of a broader study, hereafter referred to as the '*imaging dataset*'. All participants from the imaging dataset provided informed written consent in accordance with the Monash University Human Research Ethics Committee guidelines. OCD patients were recruited from specialist clinical services located in Melbourne, Australia. GD patients and HCs were recruited from the community. To be eligible for study inclusion, all participants in the imaging dataset were required to have no lifetime history of concussion, neurological disease, or drug abuse/dependence. OCD patients were required to score >8 on the severity section of the Florida Obsessive-Compulsive Inventory (FOCI; Storch et al., 2007) and have their diagnosis confirmed by treatment services as well as the Mini International Neuropsychiatric Interview version 5 conducted by L.P. and L.B. All GD patients engaged at least weekly in Electronic Gaming Machine (EGM) gambling, were required to score >8 on the Problem Gambling Severity Index (PGSI; Ferris and Wynne, 2001), and had their diagnosis confirmed by the Structured Clinical Interview for DSM-IV conducted by L.P. and L.B. The presence of either depression or anxiety, indexed by the MINI, in either OCD or GD patients was not excluded so long as the OCD and GD symptoms constituted the primary cause of distress and interference in the participant's life. Participants were excluded if they met criteria for any other psychiatric disorders, including the concurrent presence of OCD and GD.

2.2. Impulsivity and compulsivity

We measured diverse aspects of impulsivity and compulsivity using self-report indices that assessed the phenotypes as multidimensional constructs, had good validity and reliability, and were not measures of disorder-specific severity. Avoiding measures of disorder-specific symptomatology was critical to ensure we could index the full spectrum of clinical, subclinical, and healthy variation in impulsivity and compulsivity. Impulsivity was measured using the 59-item UPPS-P Impulsivity scale (Cyders et al., 2007; Whiteside and Lynam, 2001). Compulsivity was measured with the Obsessive Beliefs Questionnaire 44-item version (OBQ-44) and the 12-item version of the Intolerance of Uncertainty Scale (IUS-12) (Birrell et al., 2011; Carleton et al., 2007; Gentes and Ruscio, 2011; Myers et al., 2008; Obsessive Compulsive Cognitions Working Group, 2005).

2.3. Structural equation modelling

We modelled the dimensional structure of the self-report measures mentioned above using SEM, as per procedures described in Tiego et al. (2018). As the current study draws directly on the data used in our previous work (Tiego et al., 2018), we did not expect our model fit to change. Even so, it was prudent to re-evaluate the bifactor model under our expanded sample in order to verify its generalizability, particularly to individuals in the clinical range of symptom severity. Furthermore, since our expanded sample included participants recruited from different countries, we conducted extensive additional analysis, which we report in the supplementary material, that supported our use of a combined sample for this study. Data screening and preliminary analyses were conducted in IBM SPSS Statistics Version 23. Univariate outliers were identified and removed using a sequential fence procedure constructed using the upper and lower quartiles, defined as: $f_Q = n/4 + (1/4)$, and a 2.2 multiplicative of the interquartile range (Hoaglin and Iglewicz, 1987). All confirmatory factor analysis (CFA) models were estimated in Mplus 7.2 using the covariance matrix (Muthén and Muthén, 2012). A two-step analysis strategy was used: (i) item-level data obtained from the UPPS-P, IUS-12, OBQ-44, questionnaires were analyzed using separate first-order CFAs to determine their optimal latent structure; (ii) Factor score estimates representing individual differences on each of these first-order latent dimensions were entered as variables for estimation of the second-order dimensional phenotypes model. First-order CFA models of ordered categorical data were estimated using the Weighted Least Squares Means and Variance adjusted estimator (WLSMV) and Theta parameterization with item loadings and thresholds freely estimated and the error variance of latent response variables fixed at one (Byrne, 2012; Muthén and Muthén, 2012).

Second-order CFA of the factor score estimates generated from the first-order models were estimated using Full Information Maximum Likelihood and the Bollen-Stine Bootstrap procedure with 10,000 posterior draws (Enders, 2010; Muthén and Muthén, 2012). Latent variable scaling was performed using the fixed factor method (Byrne, 2012). *Post hoc* model fitting was performed using the Benjamini-Hochberg False Discovery Rate (FDR) and freely estimated error covariances were retained if statistically significant with the FDR set at $q = 0.05$. Model fit was assessed using a combination of absolute and incremental fit indices, including the chi square test statistic (χ^2), Root Mean Square Error of Approximation (RMSEA) ($\varepsilon < 0.05$ close approximate fit; $\varepsilon = 0.05$ - 0.10 reasonable approximate fit; $\varepsilon > 1.0$ poor fit), Comparative Fit Index (CFI) (≥ 0.90 = reasonable fit; ≥ 0.95 = good fit), and Standardized Root Mean Square Residual (SRMR; <0.08 = good fit), or Weighted Root Mean Residual (WRMR; ≤ 0.950 = good fit) for categorical variables (Bagozzi and Yi, 2011; Bentler and Bonett, 1980; Browne and Cudeck, 1993; Marsh et al., 2004; Yu, 2002). Factor score estimates were generated in Mplus using the regression method and their reliability and validity were calculated using factor score determinacy and H index values (Grice, 2001; Hancock and Mueller, 2001). The H index varies from 0 to 1, with values greater than 0.70 indicating adequate replicability of the factors across studies using the same variables. Factor score determinacies (ρ) also vary from 0 to 1, with values of approximately $\geq .9$ indicating that the factor score estimates provide a valid measure of individual differences on the corresponding latent dimensions (DiStefano et al., 2009; Grice, 2001).

2.4. Acquisition, pre-processing, denoising, and quality control of magnetic resonance imaging data

MRI data were acquired on a Siemens MAGNETOM Skyra 3T scanner. For the imaging dataset, a high-resolution anatomical image was obtained using a T1-weighted MP-RAGE structural scan (TE = 2.55 ms, TR = 1.52s, flip angle = 9°, 1 mm isotropic voxels, in-plane matrix = 192 × 240, 256 slices) and a whole-brain eyes-closed rs-fMRI sequence (7 min and 50 s) was obtained using BOLD contrast sensitive gradient echoplanar imaging (EPI) (TE = 30 ms, TR = 2.5s, flip angle = 90°, 189 vol, 3 mm isotropic voxels, in-plane matrix = 64 × 64, 44 slices acquired interleaved ascending, 3.0 mm slice thickness).

Pre-processing and quality control was performed as per Parkes et al. (2018) using Matlab code available online (https://github.com/lindenmp/rs-fMRI). Briefly, T1-weighted data were processed by removing the neck (FSL's *robustfov*), segmenting into white matter (WM), cerebrospinal fluid (CSF), and gray matter (GM) probability maps (SPM8's *New Segment*), and spatially warping the T1 and associated tissue maps to MNI space using the nonlinear deformation algorithm implemented in the Advanced Normalization Tools (ANTs; Avants, Epstein, Grossman and Gee, 2008). In order to yield more specific estimates of WM and CSF signals for subsequent denoising, we applied up to five erosion cycles to the WM mask and up to two erosion cycles to the CSF mask following extraction of the ventricles and before spatial normalization (Parkes et al., 2018; Power et al., 2017).

Prior to denoising, EPI data were processed by removing the first four volumes and applying slice-time correction (SPM8), spatial realignment (SPM8), co-registration to the T1-weighted image and nonlinear warping to MNI space using the warps derived above. . Then, EPI data were linearly detrended and spatially smoothed with a 6 mm FWHM kernel. We note that node-level time series (see below for definition) were equivalent for FWHM kernels of 4 mm and 8 mm. After smoothing, the EPI data were denoised using ICA-AROMA (Pruim, Mennes, Buitelaar and Beckmann, 2015a; Pruim, Mennes, van Rooij, Llera, Buitelaar, et al., 2015b) and regression of the mean WM/CSF signals, before being bandpass filtered (between 0.008 and 0.08 Hz) (Parkes et al., 2018). Bandpass filtering was done using fast Fourier transform and suppressing frequencies outside the bandpass range.

As per recommendations in Parkes et al. (2018), participants were excluded from analysis if any of the following were true: (i) mean framewise displacement (mFD) was >0.2 mm; (ii) FD contained >20% motion spikes, where spikes were defined as a single FD of >0.25 mm; or (iii) any FDs >5 mm. Additionally, we report the residual cross-subject correlation between FD and whole brain functional connectivity following denoising, quantified both as a percentage of connections significantly impacted by motion (i.e., QC-FC correlations), as well as the impact that distance between brain regions has on this effect (i.e., QC-FC distance-dependence).

2.5. Dynamic causal modelling

Effective connectivity was estimated using spectral DCM (spDCM) (Friston et al., 2014; Razi et al., 2015) implemented in SPM12 r7219 (Wellcome Trust Centre for Neuroimaging, London, UK; code available at: https://github.com/lindenmp/rs-fMRI/tree/master/stats/spDCM). spDCM was developed specifically for modelling rs-fMRI data and provides a computationally efficient way to estimate effective connectivity by fitting cross spectra rather than the time series (Friston et al., 2014). Owing to projections within CSTC circuitry being predominantly ipsilateral (Haber, 2003; Haber and Knutson, 2009), we estimated CSTC effective connectivity separately in each hemisphere.

2.5.1. Generation of DCM nodes

We defined functional regions of interest (ROI) that sampled key regions of the CSTC circuits implicated in impulsivity, compulsivity, GD, and OCD. The dorsal circuit comprised the dorsal striatum, anterior cingulate cortex (aCC), orbitofrontal cortex/ventromedial prefrontal cortex (OFC/vmPFC), and anterior thalamus (Fineberg et al., 2014; Gillan et al., 2015). The ventral circuit comprised the ventral striatum, aCC, OFC/vmPFC, dorsolateral prefrontal cortex (dlPFC), and posterior thalamus (Figee et al., 2013; Fineberg et al., 2014). Dorsal and ventral striatal subregions were extracted from a data-driven striatal parcellation based on structural connectivity (Parkes et al., 2017). The parcellation was cross-validated using transcriptional gene expression from the Allen Institute Human Brain Atlas (Hawrylycz et al., 2012), demonstrating its biological validity.

The anatomical brain regions for each CSTC circuit cover large parts of the brain and likely contain multiple heterogenous signals, which is not ideal for connectivity analysis. As such, each anatomical ROI outside the striatum was refined into a spherical DCM ROI with radius 3-mm using the following procedure (Heim et al., 2007). First, we mapped the seed-based functional connectivity of the dorsal and ventral striatal subregions for each subject using a whole-brain general linear model as implemented in SPM12. For each striatal subregion, subject-specific contrast images were included in a 3 × 2 factorial design (group (HC, OCD, PG) by hemisphere (left, right)). To estimate the main effect of striatal subregion at the second level, single-sample *t*-tests were run for each striatal subregion and each hemisphere separately, collapsing across all three groups. Second, anatomical masks were generated in each hemisphere using the following AAL region(s): (i) thalamus; (ii) aCC; (iii) OFC/vmPFC; and (iv) dlPFC. Third, for each striatal subregion, anatomical mask, and hemisphere, we generated a spherical search volume with a 16-mm radius (12-mm was used for the thalamus due to the smaller anatomical size of this region) centered on the maximum *t*-value from the second-level main effect. We multiplied each search volume by the corresponding anatomical mask to ensure voxels outside our anatomical regions of interest were not included. To ensure we were not capturing effects from within the striatal subregions themselves, we also removed voxels from the search volumes that were within 20-mm of the center of mass of the corresponding striatal subregion and subtracted voxels that overlapped with other search volumes (this only occurred for the aCC for the ventral CSTC circuit). This resulted in a set of search volumes for each CSTC circuit that captured the group level functional connectivity between each striatal subregion and the corresponding anatomical masks. Finally, for each subject and search volume, we found the maximal functional connectivity value (using the first-level contrast images) and generated a sphere with radius 3-mm as the DCM ROI. For each DCM ROI, time series were extracted as the principal eigenvariate of all voxel time series. It is important to note that using functional connectivity to guide DCM ROI generation in this way is not statistically circular (Stephan et al., 2010). Whereas a general linear model reveals voxels in our anatomical regions of interest that are coupled to the striatum, it tells us nothing about the mechanisms that underlie this effect. DCM is used to define a model of these mechanisms.

In summary, the above procedure resulted in subject-specific DCM ROIs with radius 3-mm that satisfied the following criteria: (i) within a 16-mm radius of the second-level main effect of striatal seed for the whole sample (12-mm for the thalamus); (ii) within the boundaries of the corresponding anatomical ROI; (iii) at least 20-mm away from the center of mass of the corresponding striatal seed; and (iv) did not overlap with DCM ROIs generated for any of the other anatomical ROIs.

2.5.2. First-level specification and inversion of DCM

For each participant and hemisphere, a sparse parent model (Fig. 1), defined *a priori,* was created that modelled connectivity from the cortical DCM ROIs to the corresponding striatal DCM ROI, from the striatal DCM ROI to the corresponding thalamic DCM ROI, and from the thalamic DCM ROI back to the corresponding cortical DCM ROIs. We excluded connections within the CSTC circuits that were not relevant to our hypotheses. Hence, cortico-cortico connections were not modelled as we were primarily interested in examining the connectivity between cortex and subcortex. This procedure was repeated for each CSTC circuit and both

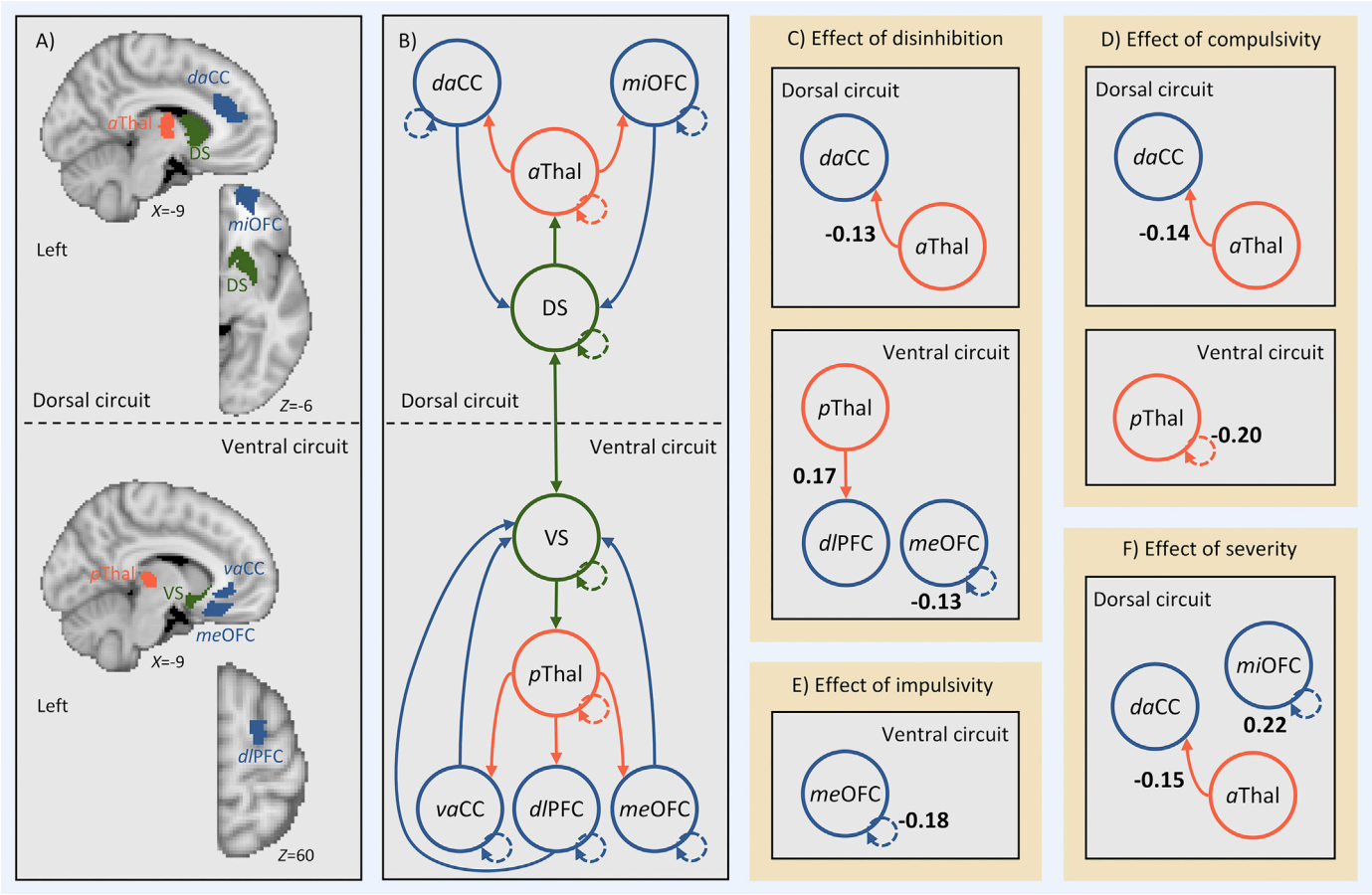

Fig. 1. Effective connectivity between regions in cortical-striatal-thalamic-cortical (CSTC) circuits covaries with individual differences in disinhibition, compulsivity, and impulsivity. Left (*A*) brain regions in the *left* hemisphere (i.e., search volumes for subject-specific DCM ROIs), and (*B*) wiring diagram representing the model that was specified. Solid lines represent connectivity between regions. Arrow heads depict direction of connection. Dashed lines represent inhibitory self-connections. Right, effects of phenotypes (*C*, *D*, and *E*) and clinical severity (*F*) on effective connectivity within CSTC circuits in the *left* hemisphere as assessed using parametric empirical Bayes. Effective connectivity parameters are described in Hz (right panel, bold numbers), where the activity in one node influences the rate of change in the activity in another. Self-connections are (log)scaled. In both cases, the interpretaion is the same, with increasing scores on a given phenotype the effective connectivity between, or the inhibitory activity within, node connectivity decreases/increases as specified. The DCM ROIs have each been labeled according to which subregions of their respective anatomical ROI they were localized to during DCM ROI generation (see method and supplementary results for details). daCC = dorsal anterior cingulate cortex, vaCC = ventral anterior cingulate cortex, miOFC = middle orbitofrontal cortex, meOFC = medial orbitofrontal cortex, aThal = anterior thalamus, pThal = posterior thalamus, dlPFC = dorsolateral prefrontal cortex, DS = dorsal striatum, VS = ventral striatum.

were combined into a single DCM. To link the two circuits, the dorsal and ventral striatal subregions were connected reciprocally. Nested models were generated by systematically turning off each of the connections present in the parent model. The parent model and nested models together formed a model space of 15 models. The parent model was inverted using spDCM (**spm_dcm_fit.m**), and the nested models were inverted using Bayesian model reduction (**spm_dcm_bmr.m**) (Friston et al., 2016). Because nested models are defined only by the removal of connections included in the parent model, they differ only in terms of their priors, which allows efficient/rapid estimation of nested DCM models by using the posterior of the parent model.

2.5.3. Second-level DCM analysis using parametric empirical Bayes

Instead of conducting a model selection process, where a single winning model is selected and applied to each participant's data, we used the parametric empirical Bayes (PEB) routines to perform second-level analysis and Bayesian model averaging (**spm_dcm_peb.m** & **spm_dcm_peb_bmc.m**). PEB is a fully Bayesian and hierarchical second-level analysis framework that, when applied to the model spaced defined above, takes into account the evidence for each connection's contribution to the DCM at the second-level. In hierarchical models, the posterior density over model parameters is constrained by the posterior from the level above. In group studies, this translates to modelling how within-subject effects relate to second-level group effects and differs from classical testing in that it considers the full posterior density over the parameters (i.e., both the expected connection strengths and their covariance from each first-level DCM). We used a pair of second-level PEB routines to examine: (1) the effects of disinhibition, impulsivity, compulsivity, and case-control/case-case comparisons on effective connectivity; and (2) the effects of clinical severity on effective connectivity.

For the first PEB model, a second-level design matrix space was defined using a constant in the first column (modelling the mean across the sample), the three phenotypes of disinhibition, impulsivity, and compulsivity, as well as covariates for age, gender, IQ, medication status (medicated/unmedicated), and mean framewise displacement (mFD), a summary measure of head motion (Parkes et al., 2018). To examine the effect of case-control/case-case comparisons on effective connectivity, we included linear contrasts for all possible combinations of our diagnostic groups (HC, OCD, and GD). We generated the following contrasts: (i) HC > OCD; (ii) HC > GD; (iii) HC < OCD; (iv) HC < GD; (v) OCD > GD; and (vi) OCD < GD. These six contrasts were input as separate columns in the design matrix of our PEB model. Finally, the above PEB model was repeated twice, once including scores on the Beck Depression Inventory (BDI) to examine the impact of depression on the results and

again including the State-Trait Anxiety Inventory (STAI) to examine the impact of anxiety.

The second PEB model retained only the OCD and GD participants and included an aggregate measure of symptom severity alongside all the same variables and contrasts from the first PEB model. We indexed clinical severity separately for the OCD and GD groups using the Obsessive-Compulsive Inventory-Revised (OCI-R; Foa et al., 2002) and the Problem Gambling Severity Index (PGSI; Ferris and Wynne, 2001), respectively. Then, as a proxy for transdiagnostic symptom severity, we *z*-scored each measure within each group separately (i.e., z-scored the PGSI across participants in the GD group and z-scored the OCI-R across participants in the OCD group), then *z*-scored again across all patients from both groups to create a single measure of severity, and included this measure in the PEB model.

3. Results

3.1. Participants and data

Of the 487 participants from the online dataset, three were excluded because of outlying scores on the phenotypes from our bifactor model (*Supplementary Results*). Of the 96 participants from the imaging dataset, one individual from the GD group was excluded due to outlying scores on phenotypes from our bifactor model (*Supplementary Results*). This yielded a final phenotype modelling sample of 579 participants, of which a subset of 39 HC participants, 34 OCD participants, and 22 GD participants underwent imaging.

Following phenotype modelling, four more individuals from the imaging dataset were excluded due to excessive motion (one from the HC group, one from OCD, and two from GD) and one individual from the OCD group was excluded due to poor EPI quality. This yielded a final imaging sample of 38 HC participants, 32 OCD participants, and 20 GD participants. See supplemental information for quality control of rs-fMRI data, and co-ordinates for ROIs. Demographics for this final imaging sample as well as the online sample are provided in Table 1. No significant differences between HC, OCD, and GD groups were observed for age, gender, IQ, or illness duration (all $p > .05$). OCD patients endorsed at least four of the six OCD symptom domains indexed by the OCI-R (i.e., Washing, Obsessing, Hoarding, Ordering, Checking, and Neutralising) with 53% of patients endorsing symptoms within all six domains.

3.2. Impulsivity and compulsivity phenotypes

We first confirmed that the bifactor model from our prior work (Tiego et al., 2018) (Fig. S1, *Supplement*) provided the best fit (χ^2 (31) = 52.903, $p = .057$; RMSEA = 0.035; 90% *CI* = 0.018 - 0.50; CFI = 0.99; SRMR = 0.041) to this new, extended dataset, relative to several competing models (Table S2, *Supplement*). We then generated factor score estimates for each of the three phenotypes for subsequent analyses. The distributions of the factor score estimates were univariate and multivariate normal, providing evidence for a continuous distribution for the disinhibition, impulsivity, and compulsivity phenotypes that spans the non-clinical and clinical spectrum.

Next, we examined whether clinical GD and OCD participants lie at the extreme ends of our phenotypes. A MANOVA revealed significant differences between non-clinical (i.e., the online dataset combined with the HCs from the imaging dataset), OCD and GD participants (Pillai's = 0.110, F (6,1150) = 11.164, $p < .001$; $\eta^2_p = 0.055$, on the disinhibition (F (2,576) = 21.197, $p < .001$, $\eta^2_p = 0.071$), impulsivity (F (2,576) = 10.210, $p < .001$, $\eta^2_p = 0.034$), and compulsivity (F (2,576) = 3.304, $p = .037$, $\eta^2_p = 0.011$) phenotypes. Pairwise *post hoc* comparisons corrected using the Benjamini-Hochberg False Discovery Rate (FDR, $q = 0.05$) (Benjamini and Hochberg, 1995) revealed that the OCD ($\Delta M = 0.917$, $SE = 0.167$, 95%$CI = 0.589–1.244$, $p < .001$) and GD participants ($\Delta M = 0.809$, $SE = 0.205$, 95%$CI = 0.407–1.211$, $p < .001$) were significantly higher on disinhibition than non-clinical participants; GD participants were higher on impulsivity than non-clinical participants ($\Delta M = 0.697$, $SE = 0.190$, 95%$CI = 0.352–1.069$, $p < .001$) and OCD participants ($\Delta M = 1.073$, $SE = 0.238$, 95%$CI = 0.605–1.541$, $p < .001$); and OCD participants were higher on compulsivity than GD participants ($\Delta M = 0.590$, $SE = 0.294$, 95%$CI = 0.101–1.079$, $p = .023$), but not the non-clinical participants ($\Delta M = 0.118$, $SE = 0.164$, 95%CI = -0.204 – 0.441, $p = .585$). The lack of significant difference between OCD and the non-clinical participants is due to the presence of higher compulsivity in individuals within the online dataset. Repeating the above analysis separating the HCs in the imaging dataset from the online dataset revealed that OCD participants had significantly higher compulsivity scores than the HCs ($\Delta M = 0.461$, $SE = 0.217$, 95%CI = 0.035-0.887, $p = .034$), but not the online dataset ($\Delta M = 0.091$, $SE = 0.164$, 95% CI = -0.231-0.413, $p = .580$), and that the online dataset had higher compulsivity compared to HCs ($\Delta M = 0.370$, $SE = 0.154$, 95% $CI = 0.068–0.672$, $p = .016$). The full distributions of the phenotype scores are presented in Fig. S3 and show the considerable range of psychopathology in the online sample. These results thus support the success of our strategy to use the online group to sample a broader range of psychopathological severity than the highly-screened MRI healthy control group.

Table 1
Sample characteristics.

Characteristic	HC (n = 38)	OCD (n = 32)	GD (n = 20)	Online cohort (n = 487)
Age in years, mean (SD)	34 (9.17)	32.34 (9.26)	34.50 (11.25)	34.2 (9.30)
Male, No. (%)	19 (48)	15 (47)	13 (65)	240 (49)
IQ, mean (SD)	115.26 (10.79)	115.62 (8.99)	110.45 (8.39)	–
SSRI Medication, No. (%)	0 (0)	19 (59)	4 (20)	–
Illness duration in years (SD)	–	12.09 (7.78)	8.38 (6.32)	–

Note, online cohort is the same as used in Tiego et al. (2018). HC = Healthy control; OCD = Obsessive-compulsive disorder; GD = Gambling disorder; IQ = Intelligence quotient; SSRI = Selective serotonin reuptake inhibitor.

3.3. Effective connectivity

Having demonstrated support for the continuity hypothesis, we examined associations between scores on the disinhibition, impulsivity, and compulsivity phenotypes and CSTC effective connectivity in the imaging dataset. For all analyses, we thresholded the effective connectivity results using a posterior probability of >95%. In general, we found that the effects of phenotypic variation on effective connectivity between regions was lateralized to the left hemisphere, with effects in the right hemisphere only observed on the inhibitory self-connections of regions. We present effects from the left hemisphere in the main text. Results for the right hemisphere are found in Fig. S4.

Fig. 1 shows the effect of each phenotype on effective connectivity, whilst controlling for the effects of the nuisance covariates, diagnostic contrasts, and the other phenotypes. Fig. 1 shows that individuals with higher scores on disinhibition exhibited (i) lower bottom-up effective connectivity from the left anterior thalamus to the left dorsal aCC (daCC) in the dorsal circuit; (ii) greater bottom-up effective connectivity from the left posterior thalamus to the left dlPFC in the ventral circuit; and (iii) lower inhibitory activity in the self-connection for the medial OFC (meOFC) in the ventral circuit. Individuals with higher levels of compulsivity exhibited (i) lower bottom-up effective connectivity from the left anterior thalamus to the left daCC in the dorsal circuit; and (ii) lower inhibitory activity in the self-connection for the posterior thalamus in the ventral circuit. Individuals with high impulsivity showed no differences in effective connectivity. Instead, they showed lower inhibitory activity in the self-connection for the medial OFC (meOFC) in the ventral

circuit. When effects of diagnostic category were included in the full model that also accounted for the effects of our dimensional phenotypes, no effects were observed for any case-control or case-case contrasts. This result indicates that diagnostic differences did not account for additional variance in effective connectivity beyond the dimensional constructs. When repeating the analysis with a model that included only diagnosis and nuisance covariates with no dimensional constructs, we found significant effects of diagnosis on bottom-up CSTC signalling that overlapped with the results reported in Fig. 1. In particular, patients exhibited lower bottom-up effective connectivity from the left anterior thalamus to the left daCC in the dorsal circuit and higher bottom-up effective connectivity from the left posterior thalamus to the left dlPFC in the ventral circuit compared to HCs. Together these results indicate that any apparent differences between diagnostic groups are driven by quantitative variation in dimensional phenotypes, rather than qualitative distinctions between traditional diagnostic categories. A complementary analysis using traditional frequentist as well as Bayesian analysis applied to estimates of undirected functional connectivity yielded largely null findings, demonstrating the sensitivity of our analysis of effective connectivity (*Supplementary Results*).

Second, we examined the effect of controlling for depression and anxiety (indexed via the BDI and the STAI, respectively) on the above results. When including BDI in the PEB model, the effects reported above for the phenotypes remained. However, when including STAI in the PEB model, the effects for disinhibition were absent under the posterior probability of >95% but were present under a posterior probability of >75%, suggesting some of the variance in effective connectivity explained by disinhibition was accounted for by anxiety. The effects observed for compulsivity and impulsivity remained when including STAI in the PEB model, indicating that these effects are independent.

Lastly, we examined the effect of clinical severity on effective connectivity in the OCD and GD patients. Consistent with the effects of disinhibition and compulsivity, symptom severity was associated with lower bottom-up effective connectivity from the left anterior thalamus to the left daCC in the dorsal circuit (Fig. 1). The effects of disinhibition and compulsivity reported above remained when controlling for the effect of severity, indicating that both clinical severity and dimensional phenotypes make independent contributions to thalamo-cingulate connectivity. Greater severity was also associated with greater inhibitory activity in the self-connection for the middle OFC (miOFC) in the dorsal circuit.

4. Discussion

The potential benefits of understanding the neurobiology of quantitative traits that underlie risk for mental illness are widely acknowledged, and underpin the RDoC model (Cuthbert and Insel, 2013; Insel et al., 2010). Here, we first characterized the dimensional structure of impulsivity and compulsivity in a sample of non-clinical individuals and people with clinically diagnosed OCD and GD, and then examined how effective connectivity within CSTC circuitry relates to quantitative variation in these dimensional traits. Complementing our earlier work (Tiego et al., 2018), we find that variance in a broad battery of impulsive and compulsive self-report measures is best explained by a bifactor model, comprising a unitary disinhibition factor with loadings from nearly all scales, coupled with specific constructs capturing residual variance in impulsivity and compulsivity. While this result is not entirely surprising given the large overlap between the data examined in Tiego et al. (2018) and the data examined in the current study, our results show that our bifactor model is not limited to describing subclinical variation in impulsivity and compulsivity and is able to characterize the full spectrum of variability. Critically, we report that high levels of disinhibition and compulsivity correlate with altered bottom-up signalling from subcortical to cortical areas in dorsal and ventral CSTC systems, and that variance in effective connectivity was better explained by quantitative, transdiagnostic variation in these constructs than traditional diagnostic categories. Together, our results support the utility of using dimensional constructs that cut across traditional diagnostic boundaries for understanding pathophysiological processes in psychiatry. Our use of DCM to distinguish between directional influences in CSTC circuitry also suggests that the pathological expression of these dimensional traits may be related to altered subcortical signalling to cortical regions (Fineberg et al., 2010, 2014).

4.1. Disinhibition, impulsivity, compulsivity and the continuum model

We previously validated a model in a large online normative sample and found that various measures of impulsivity and compulsivity were best represented by three empirically-distinct phenotypes of disinhibition, impulsivity, and compulsivity (Tiego et al., 2018). Furthermore, we demonstrated that these phenotypes explained subclinical variation in a broad range of impulsive, addictive, and obsessive-compulsive symptomatology (Tiego et al., 2018). Here, we extended these findings by applying the model to an expanded sample that also included individuals with diagnosed GD and OCD. We show that a bifactor model comprising disinhibition, impulsivity, and compulsivity constructs remains the best fit to the data supporting the robustness of the previously proposed model. Furthermore, OCD and GD groups generally sat on the extreme ends of traits that had univariate and multivariate normal distributions (see Fig. S3), supporting a continuum model in which disorder represents the extreme expression of traits with a continuous population distribution. In particular, both OCD and GD showed higher scores on the disinhibition phenotype compared to the HCs, OCD patients showed higher compulsivity relative to HCs, and GD patients showed higher impulsivity relative to HCs.

The GD group showed lower scores on the compulsivity phenotype than compared to HCs, which runs counter to the literature demonstrating higher compulsivity in the GD population (van Timmeren et al., 2018). We note however that our compulsivity dimension captures variance specific to compulsivity measures after accounting for any shared variance with impulsivity, which is captured by our disinhibition phenotype. The fact that GD individuals show higher scores on the disinhibition construct but not compulsivity suggests that prior reports of greater compulsivity in GD may be explained by phenotypic variance that is shared with impulsivity, rather than compulsivity specifically. Our findings also suggest that our compulsivity dimension represents aspects of compulsivity that are selectively higher in OCD but lower in GD. This may relate to differences in measurement. Indeed, we used self-report data in the current study while much of the extant GD literature has focused on the cognitive aspects of compulsivity (van Timmeren et al., 2018). Overall, our results are in line with the basic premise of the RDoC initiative, and support characterization of the full range of variation between normal and abnormal functioning as a critical first step to developing individually targeted treatment strategies in psychiatry (Cuthbert and Insel, 2013).

4.2. Quantitative traits covary with bottom-up signalling in CSTC circuitry

Higher scores on the disinhibition dimension correlated with lower resting-state bottom-up connectivity in the dorsal circuit and greater bottom-up connectivity in the ventral circuit. These findings demonstrate that higher levels of impulsivity, uncertainty intolerance, and obsessive beliefs, in conjunction with lower levels of desire for predictability, perfectionism, and threat estimation are associated with divergent changes across distinct CSTC circuits. Our results are the first to demonstrate that dysfunction in these aspects of impulsivity and compulsivity may be associated with a dysfunctional behavioral drive subserved by the subcortical components of the CSTC circuits (Fineberg et al., 2010, 2014). Previous resting-state work using functional connectivity has shown higher levels of ventral CSTC connectivity in both OCD and GD (Figee et al., 2013; Harrison et al., 2013; Koehler et al., 2013), which is reduced in OCD via deep brain stimulation to the ventral striatum (Figee et al., 2013). Our results suggest that this effect may arise

through the remediation of excessive bottom-up connectivity in the ventral CSTC circuit.

We also found that higher scores on the compulsivity-specific dimension correlated with reductions in resting-state bottom-up connectivity in the dorsal CSTC circuit. This result appears counter to previous task-based fMRI studies showing dorsal striatum hyperactivation and greater functional connectivity with the ACC in OCD patients who develop compulsive habits relative to those who do not (Gillan et al., 2015). This apparent discrepancy may be related to the use of task-based versus resting-state fMRI protocols. Gillan et al. (2015) explain dorsal CSTC dysfunction as a deficit in goal-directed control over behavior, which leads to an over-reliance on habits. Our resting-state design did not overtly engage goal-driven behavioral systems. Hence, dysfunction in the dorsal CSTC circuit may be context-specific, such that connectivity is greater when compulsive behavior is expressed but lower at rest. Concurrent modelling of effective connectivity during task and rest could be used to test this hypothesis in future.

Additionally, effects in the dorsal circuit that overlapped with those found for disinhibition and compulsivity were also observed with increasing clinical severity, demonstrating that the variation in effective connectivity explained by our phenotypes was clinically relevant. Finally, we found that our results were largely constrained to the left hemisphere, suggesting a lateralization of effects (see *Supplementary Results* for results in the right hemisphere). Despite previous reports of lateralization of dysconnectivity in both OCD (Harrison et al., 2013) and GD groups (Jung et al., 2014), the precise reasons for lateralization is unclear and remains a topic for further investigation.

4.3. The utility of effective connectivity models

Functional connectivity estimates undirected coupling between measured neurophysiological signals, whereas effective connectivity is based on a model of the causal interactions between neuronal populations that drive the measured signals (Friston et al., 2003). Previous research has shown effective connectivity is more sensitive to age-related changes than functional connectivity (Tsvetanov et al., 2016). Indeed, effective connectivity should offer a more precise characterization of pathophysiological processes that is less susceptible to various nuisance factors that can contaminate measures of functional connectivity (Friston, 2011). Here, we combined estimates of effective connectivity (Friston et al., 2014) with a fully Bayesian analysis framework (Friston et al., 2016). While the application of these methods in psychiatry is growing, so far they have been predominantly applied to schizophrenia (Friston et al., 2016; Stephan et al., 2015; Zhou et al., 2018). Thus, to demonstrate the utility of DCM in psychiatry, we replicated our analyses using functional connectivity and found no associations that survived correction for multiple comparisons. Our results thus support the superior sensitivity of a fully Bayesian analysis of effective connectivity for uncovering brain-behavior relationships in psychiatry.

4.4. Limitations

Head motion is a pernicious issue in rs-fMRI data (Ciric et al., 2017; Power et al., 2015; Satterthwaite et al., 2012) that confounds pathophysiological inferences (Parkes et al., 2018). To rigorously address this issue, we adopted state-of-the-art denoising methods (Pruim, Mennes, Buitelaar and Beckmann, 2015a; Pruim, Mennes, van Rooij, Llera, Buitelaar, et al., 2015b) and stringent participant exclusion criteria (Parkes et al., 2018; Satterthwaite et al., 2013) that minimized motion-related confound in our data. Our cross-sectional design is another limitation given that OCD and GD patients may express different levels of impulsivity and compulsivity throughout the course of their illness (Fontenelle et al., 2011). Longitudinal investigations could clarify how latent phenotypes and their neural substrates change over time. More than half of our OCD patients and four of the GD patients were on SSRI medication. Covarying for medication status had no impact on our findings, and to our knowledge the precise effects of SSRIs on CSTC effective connectivity have not been investigated. Although these analyses suggest a minimal effect of medication, the modest size of our clinical groups means that our results will benefit from replication in other datasets.

We found that controlling for anxiety reduced the effect of disinhibition on the dorsal and ventral circuits, suggesting that these results were partially accounted for by anxiety. However, the effects for compulsivity and impulsivity remained. We selected the OBQ-44 and IUS-12 as our measures of compulsivity. Compulsivity as a construct in its own right has been investigated less compared to impulsivity in the extant literature. While previous work has chosen to index compulsivity in terms of disorder-specific compulsive behaviours (Chamberlain et al., 2017), here we opted instead to focus on aspects of compulsivity that may better characterize the full range of compulsivity in the population. As such, our compulsivity dimension was biased towards the obsessional and cognitive aspects of compulsivity. Future work may evaluate how more specific compulsive behaviours relate to effective connectivity in CSTC circuits.

5. Conclusions

Intermediate phenotypes are viewed as a promising method for understanding behavioral and biological mechanisms of risk for diverse disorders (Cuthbert and Insel, 2013; Hyman, 2007; Insel et al., 2010). We show that dimensional constructs related to impulsivity and compulsivity more closely track neuronal dynamics within cortico-striatal-thalamic-cortical circuits than the traditional diagnostic categories of OCD and GD. We also show that model-based estimates of effective connectivity successfully differentiate top-down and bottom-up dynamics, whereas estimates of functional connectivity yield largely null results. These findings suggest that Bayesian analysis of effective connectivity may provide a valuable tool for identifying biomarkers that cut across diagnostic boundaries.

Author contributions

L. P., J. T., K. A., A. F., and M. Y. designed research; L. P. performed research; L. P. contributed unpublished reagents/analytic tools; L. P., J. T., K. A., A. F., B. P., and A. R. analyzed data; L. P., J. T., K. A., L. B., S. R. C., L. F., B. J. H., V. L., B. P., A. R., A. F., and M. Y. wrote the paper.

Competing interests

S.R.C consults for Cambridge Cognition, Shire, and Promentis. The remaining authors declare no competing financial interests.

Acknowledgements

We sincerely thank Dr. Ben Fulcher for his input in early phases of project planning and development of ideas. L.P. was supported by an Australian Postgraduate Award. J.T. was supported by National Health and Medical Research Council (ID:1002458, 1046054). A.F. was supported by the Charles and Sylvia Viertel Foundation, the Australian Research Council (ID: FT130100589) and the National Health and Medical Research Council (ID: 3251213, 3251250, 3251392). M.Y. was supported by a National Health and Medical Research Council Fellowship (ID: 1117188), Monash University and the David Winston Turner Endowment Fund. B.H was supported by a National Health and Medical Research Council Fellowship (ID: 1124472). A.R. was funded by Australian Research Council DECRA Fellowship (Ref: DE170100128) and the Wellcome Trust.

Appendix A. Supplementary data

Supplementary data to this article can be found online at https://doi.org/10.1016/j.neuroimage.2019.116070.

References

Anderson, K.M., Krienen, F.M., Choi, E.Y., Reinen, J.M., Yeo, B.T.T., Holmes, A.J., 2018. Gene expression links functional networks across cortex and striatum. Nat. Commun. 9 (1), 1–14. http://doi.org/10.1038/s41467-018-03811-x.

Avants, B., Epstein, C., Grossman, M., Gee, J., 2008. Symmetric diffeomorphic image registration with cross-correlation: evaluating automated labeling of elderly and neurodegenerative brain. Med. Image Anal. 12 (1), 26–41. http://doi.org/10.1016/j.media.2007.06.004.

Bagozzi, R.P., Yi, Y., 2011. Specification, evaluation, and interpretation of structural equation models. J. Acad. Mark. Sci. 40 (1), 8–34. http://doi.org/10.1007/s11747-011-0278-x.

Balodis, I.M., Kober, H., Worhunsky, P.D., Stevens, M.C., Pearlson, G.D., Potenza, M.N., 2012. Diminished frontostriatal activity during processing of monetary rewards and losses in pathological gambling. Bps 71 (8), 749–757. http://doi.org/10.1016/j.biopsych.2012.01.006.

Benjamini, Y., Hochberg, Y., 1995. Controlling the False Discovery rate: a practical and powerful approach to multiple testing. J. R. Stat. Soc. Ser. B 57 (1), 289–300.

Bentler, P.M., Bonett, D.G., 1980. Significance tests and goodness of fit in the analysis of covariance structures. Psychol. Bull. 88 (3), 588–606. http://doi.org/10.1037/0033-2909.88.3.588.

Birrell, J., Meares, K., Wilkinson, A., Freeston, M., 2011. Toward a definition of intolerance of uncertainty: a review of factor analytical studies of the Intolerance of Uncertainty Scale. Clin. Psychol. Rev. 31 (7), 1198–1208. http://doi.org/10.1016/j.cpr.2011.07.009.

Browne, M.W., Cudeck, R., 1993. Alternative ways of assessing model fit. In: Testing Structural Equation Models, pp. 136–162 (Newbury Park, CA).

Byrne, B.M., 2012. Structural Equation Modeling with Mplus: Basic Concepts, Applications, and Programming. Routledge, New York.

Carleton, R.N., Norton, M.A.P.J., Asmundson, G.J.G., 2007. Fearing the unknown: a short version of the intolerance of uncertainty scale. J. Anxiety Disord. 21 (1), 105–117. http://doi.org/10.1016/j.janxdis.2006.03.014.

Chamberlain, S.R., Stochl, J., Redden, S.A., Grant, J.E., 2017. Latent traits of impulsivity and compulsivity: toward dimensional psychiatry. Psychol. Med. 13, 1–12. http://doi.org/10.1017/S0033291717002185.

Choi, J.-S., Shin, Y.-C., Jung, W.H., Jang, J.H., Kang, D.-H., Choi, C.-H., et al., 2012. Altered brain activity during reward anticipation in pathological gambling and obsessive-compulsive disorder. PLoS One 7 (9) e45938–8. http://doi.org/10.1371/journal.pone.0045938.

Ciric, R., Wolf, D.H., Power, J.D., Roalf, D.R., Baum, G., Ruparel, K., et al., 2017. Benchmarking of participant-level confound regression strategies for the control of motion artifact in studies of functional connectivity. Neuroimage 1–22. http://doi.org/10.1016/j.neuroimage.2017.03.020.

Clark, L., Limbrick-Oldfield, E.H., 2013. Disordered gambling: a behavioral addiction. Curr. Opin. Neurobiol. 23 (4), 655–659. http://doi.org/10.1016/j.conb.2013.01.004.

Cuthbert, B.N., Insel, T.R., 2013. Toward the future of psychiatric diagnosis: the seven pillars of RDoC. BMC Med. 11 (1), 1–8. http://doi.org/10.1186/1741-7015-11-126.

Cyders, M.A., Coskunpinar, A., 2011. Measurement of constructs using self-report and behavioral lab tasks: is there overlap in nomothetic span and construct representation for impulsivity? Clin. Psychol. Rev. 31 (6), 965–982. http://doi.org/10.1016/j.cpr.2011.06.001.

Cyders, M.A., Smith, G.T., Spillane, N.S., Fischer, S., Annus, A.M., Peterson, C., 2007. Integration of impulsivity and positive mood to predict risky behavior: development and validation of a measure of positive urgency. Psychol. Assess. 19 (1), 107–118. http://doi.org/10.1037/1040-3590.19.1.107.

Dalley, J.W., Everitt, B.J., Robbins, T.W., 2011. Impulsivity, compulsivity, and top-down cognitive control. Neuron 69 (4), 680–694. http://doi.org/10.1016/j.neuron.2011.01.020.

DiStefano, C., Zhu, M., Mîndrilă, D., 2009. Understanding and using factor scores: considerations for the applied researcher. Pract. Assess. Res. Eval. 14 (20), 1–11.

Enders, C.K., 2010. Applied Missing Data Analysis. Guilford Press.

Everitt, B.J., Robbins, T.W., 2005. Neural systems of reinforcement for drug addiction: from actions to habits to compulsion. Nat. Neurosci. 8 (11), 1481–1489. http://doi.org/10.1038/nn1579.

Everitt, B.J., Robbins, T.W., 2013. From the ventral to the dorsal striatum: devolving views of their roles in drug addiction. Neurosci. Biobehav. Rev. 1–9. http://doi.org/10.1016/j.neubiorev.2013.02.010.

Everitt, B.J., Belin, D., Economidou, D., Pelloux, Y., Dalley, J.W., Robbins, T.W., 2008. Neural mechanisms underlying the vulnerability to develop compulsive drug-seeking habits and addiction. Philos. Trans. R. Soc. Biol. Sci. 363 (1507), 3125–3135. http://doi.org/10.1098/rstb.2008.0089.

Ferris, J.A., Wynne, H.J., 2001. The Canadian Problem Gambling Index. Ottawa, ON.

Figee, M., Luigjes, J., Smolders, R., Valencia-Alfonso, C.-E., van Wingen, G., de Kwaasteniet, B., et al., 2013. Deep brain stimulation restores frontostriatal network activity in obsessive-compulsive disorder. Nat. Neurosci. 16 (4), 386–387. http://doi.org/10.1038/nn.3344.

Fineberg, N.A., Chamberlain, S.R., Goudriaan, A.E., Stein, D.J., Vanderschuren, L.J.M.J., Gillan, C.M., et al., 2014. New developments in human neurocognition: clinical, genetic, and brain imaging correlates of impulsivity and compulsivity. CNS Spectr. 19 (01), 69–89. http://doi.org/10.1017/S1092852913000801.

Fineberg, N.A., Potenza, M.N., Chamberlain, S.R., Berlin, H.A., Menzies, L., Bechara, A., et al., 2010. Probing compulsive and impulsive behaviors, from animal models to endophenotypes: a narrative review. Neuropsychopharmacology 35 (3), 591–604. http://doi.org/10.1038/npp.2009.185.

Foa, E.B., Huppert, J.D., Leiberg, S., Langner, R., Kichic, R., Hajcak, G., Salkovskis, P.M., 2002. The Obsessive-Complusive Inventory: development and validation of a short version. Psychol. Assess. 14 (4), 485–495. http://doi.org/10.1037//1040-3590.14.4.485.

Fontenelle, L.F., Oostermeijer, S., Harrison, B.J., Pantelis, C., Yücel, M., 2011. Obsessive-compulsive disorder, impulse control disorders and drug addiction. Drugs 71 (7), 827–840. http://doi.org/10.2165/11591790-000000000-00000.

Friston, K.J., 2011. Functional and effective connectivity: a review. Brain Connect. 1 (1), 13–36. http://doi.org/10.1089/brain.2011.0008.

Friston, K.J., Harrison, L., Penny, W., 2003. Dynamic causal modelling. Neuroimage 19 (4), 1273–1302. http://doi.org/10.1016/S1053-8119(03)00202-7.

Friston, K.J., Kahan, J., Biswal, B., Razi, A., 2014. A DCM for resting state fMRI. Neuroimage 94, 396–407. http://doi.org/10.1016/j.neuroimage.2013.12.009.

Friston, K.J., Litvak, V., Oswal, A., Razi, A., Stephan, K.E., van Wijk, B.C.M., et al., 2016. Bayesian model reduction and empirical Bayes for group (DCM) studies. Neuroimage 128, 413–431. http://doi.org/10.1016/j.neuroimage.2015.11.015.

Gentes, E.L., Ruscio, A.M., 2011. A meta-analysis of the relation of intolerance of uncertainty to symptoms of generalized anxiety disorder, major depressive disorder, and obsessive–compulsive disorder. Clin. Psychol. Rev. 31 (6), 923–933. http://doi.org/10.1016/j.cpr.2011.05.001.

Gillan, C.M., Apergis-Schoute, A.M., Morein-Zamir, S., Urcelay, G.P., Sule, A., Fineberg, N.A., et al., 2015. Functional neuroimaging of avoidance habits in obsessive-compulsive disorder. Am. J. Psychiatry 172 (3), 284–293. http://doi.org/10.1176/appi.ajp.2014.14040525.

Gillan, C.M., Kosinski, M., Whelan, R., Phelps, E.A., Daw, N.D., 2016a. Characterizing a psychiatric symptom dimension related to deficits in goal-directed control. eLife 5 e94778–24. http://doi.org/10.7554/eLife.11305.

Gillan, C.M., Robbins, T.W., Sahakian, B.J., van den Heuvel, O.A., van Wingen, G., 2016b. The role of habit in compulsivity. Eur. Neuropsychopharmacol. 1–13. http://doi.org/10.1016/j.euroneuro.2015.12.033.

Gillan, C.M., Morein-Zamir, S., Urcelay, G.P., Sule, A., Voon, V., Apergis-Schoute, A.M., et al., 2014. Enhanced avoidance habits in obsessive-compulsive disorder. Bps 75 (8), 631–638. http://doi.org/10.1016/j.biopsych.2013.02.002.

Gillan, C.M., Papmeyer, M., Morein-Zamir, S., Sahakian, B.J., Fineberg, N.A., Robbins, T.W., de Wit, S., 2011. Disruption in the balance between goal-directed behavior and habit learning in obsessive-compulsive disorder. Am. J. Psychiatry 168 (7), 718–726. http://doi.org/10.1176/appi.ajp.2011.10071062.

Goudriaan, A.E., Oosterlaan, J., de Beurs, E., van den Brink, W., 2004. Pathological gambling: a comprehensive review of biobehavioral findings. Neurosci. Biobehav. Rev. 28 (2), 123–141. http://doi.org/10.1016/j.neubiorev.2004.03.001.

Grassi, G., Pallanti, S., Righi, L., Figee, M., Mantione, M., Denys, D., et al., 2015. Think twice: impulsivity and decision making in obsessive-compulsive disorder. J. Behav. Addict. 4 (4), 263–272. http://doi.org/10.1556/2006.4.2015.039.

Grice, J.W., 2001. Computing and evaluating factor scores. Psychol. Methods 6 (4), 430–450. http://doi.org/10.1037/1082-989X.6.4.430.

Gürsel, D.A., Avram, M., Sorg, C., Brandl, F., Koch, K., 2018. Frontoparietal areas link impairments of large-scale intrinsic brain networks with aberrant fronto-striatal interactions in OCD: a meta-analysis of resting-state functional connectivity. Neurosci. Biobehav. Rev. 87, 151–160. https://doi.org/10.1016/j.neubiorev.2018.01.016.

Haber, S.N., 2003. The primate basal ganglia: parallel and integrative networks. J. Chem. Neuroanat. 26 (4), 317–330. http://doi.org/10.1016/j.jchemneu.2003.10.003.

Haber, S.N., Knutson, B., 2009. The reward circuit: linking primate anatomy and human imaging. Neuropsychopharmacology 35 (1), 4–26. http://doi.org/10.1038/npp.2009.129.

Hancock, G.R., Mueller, R.O., 2001. Rethinking construct reliability within latent variable systems. In: Structural Equation Modeling Present and Future - A Festchrift in Honor of Karl Joreskog, pp. 195–216 (Lincolnwood, IL).

Harrison, B.J., Pujol, J., Cardoner, N., Deus, J., Alonso, P., López-Solà, M., et al., 2013. Brain corticostriatal systems and the major clinical symptom dimensions of obsessive-compulsive disorder. Bps 73 (4), 321–328. http://doi.org/10.1016/j.biopsych.2012.10.006.

Harrison, B.J., Soriano-Mas, C., Pujol, J., Ortiz, H., L pez-Sol, M., Hern ndez-Ribas, R., et al., 2009. Altered corticostriatal functional connectivity in obsessive-compulsive disorder. Arch. Gen. Psychiatr. 66 (11), 1189–12. http://doi.org/10.1001/archgenpsychiatry.2009.152.

Hawrylycz, M.J., Lein, E.S., Guillozet-Bongaarts, A.L., Shen, E.H., Ng, L., Miller, J.A., et al., 2012. An anatomically comprehensive atlas of the adult human brain transcriptome. Nat. Publ. Group 489 (7416), 391–399. http://doi.org/10.1038/nature11405.

Heim, S., Eickhoff, S.B., Ischebeck, A.K., Friederici, A.D., Stephan, K.E., Amunts, K., 2007. Effective connectivity of the left BA 44, BA 45, and inferior temporal gyrus during lexical and phonological decisions identified with DCM. Hum. Brain Mapp. 30 (2), 392–402. http://doi.org/10.1002/hbm.20512.

Hoaglin, D.C., Iglewicz, B., 1987. Fine-tuning some resistant rules for outlier labeling. J. Am. Stat. Assoc. 82 (400), 1147–1149. http://doi.org/10.1080/01621459.1987.10478551.

Hollander, E., 1993. Obsessive-compulsive spectrum disorders: an overview. Psychiatr. Ann. 23 (7), 355–358. http://doi.org/10.3928/0048-5713-19930701-05.

Hollander, E., Benzaquen, S.D., 1997. The obsessive-compulsive spectrum disorders. Int. Rev. Psychiatry 9 (1), 99–110. http://doi.org/10.1080/09540269775628.

Hyman, S.E., 2007. Can neuroscience be integrated into the DSM-V? Nat. Rev. Neurosci. 8 (9), 725–732. http://doi.org/10.1038/nrn2218.

Insel, T., Cuthbert, B., Garvey, M., Heinssen, R., Pine, D.S., Quinn, K., et al., 2010. Research domain criteria (RDoC): toward a new classification framework for research

on mental disorders. Am. J. Psychiatry 167 (7), 748–751. http://doi.org/10.1176/appi.ajp.2010.09091379.
Jung, M.H., Kim, J.-H., Shin, Y.-C., Jung, W.H., Jang, J.H., Choi, J.-S., et al., 2014. Decreased connectivity of the default mode network in pathological gambling: a resting state functional MRI study. Neurosci. Lett. 583, 120–125. http://doi.org/10.1016/j.neulet.2014.09.025.
Jung, W.H., Yücel, M., Yun, J.-Y., Yoon, Y.B., Cho, K.I.K., Parkes, L., et al., 2016. Altered functional network architecture in orbitofronto-striato-thalamic circuit of unmedicated patients with obsessive-compulsive disorder. Hum. Brain Mapp. 38 (1), 109–119. http://doi.org/10.1002/hbm.23347.
Koehler, S., Ovadia-Caro, S., van der Meer, E., Villringer, A., Heinz, A., Romanczuk-Seiferth, N., Margulies, D.S., 2013. Increased functional connectivity between prefrontal cortex and reward system in pathological gambling. PLoS One 8 (12) e84565–13. http://doi.org/10.1371/journal.pone.0084565.
Limbrick-Oldfield, E.H., van Holst, R.J., Clark, L., 2013. Fronto-striatal dysregulation in drug addiction and pathological gambling: consistent inconsistencies? Ynicl 2, 385–393. http://doi.org/10.1016/j.nicl.2013.02.005.
Marsh, H.W., Hau, K.-T., Wen, Z., 2004. In search of golden rules: comment on hypothesis-testing approaches to setting cutoff values for fit indexes and dangers in overgeneralizing hu and bentler's (1999) findings. Struct. Equ. Model.: Multidiscipl. J. 11 (3), 320–341. http://doi.org/10.1207/s15328007sem1103_2.
Muthén, L.K., Muthén, B.O., 2012. Mplus User's Guide, 7 ed. Muthén & Muthén, Los Angeles, CA.
Myers, S.G., Fisher, P.L., Wells, A., 2008. Belief domains of the Obsessive Beliefs Questionnaire-44 (OBQ-44) and their specific relationship with obsessive–compulsive symptoms. J. Anxiety Disord. 22 (3), 475–484. http://doi.org/10.1016/j.janxdis.2007.03.012.
Obsessive Compulsive Cognitions Working Group, 2005. Psychometric validation of the obsessive belief questionnaire and interpretation of intrusions inventory—Part 2: factor analyses and testing of a brief version. Behav. Res. Ther. 43 (11), 1527–1542. http://doi.org/10.1016/j.brat.2004.07.010.
Parkes, L., Fulcher, B.D., Yücel, M., Fornito, A., 2017. Transcriptional signatures of connectomic subregions of the human striatum. Genes Brain Behav. 25, 1176–17. http://doi.org/10.1111/gbb.12386.
Parkes, L., Fulcher, B., Yücel, M., Fornito, A., 2018. An evaluation of the efficacy, reliability, and sensitivity of motion correction strategies for resting-state functional MRI. Neuroimage 171, 415–436. http://doi.org/10.1016/j.neuroimage.2017.12.073.
Peters, J., Miedl, S.F., Büchel, C., 2013. Elevated functional connectivity in a striatal-amygdala circuit in pathological gamblers. PLoS One 8 (9) e74353–e74357. http://doi.org/10.1371/journal.pone.0074353.
Power, J.D., Plitt, M., Kundu, P., Bandettini, P.A., Martin, A., 2017. Temporal interpolation alters motion in fMRI scans: magnitudes and consequences for artifact detection. PLoS One 12 (9) e0182939–20. http://doi.org/10.1371/journal.pone.0182939.
Power, J.D., Schlaggar, B.L., Petersen, S.E., 2015. Recent progress and outstanding issues in motion correction in resting state fMRI. Neuroimage 105, 536–551. http://doi.org/10.1016/j.neuroimage.2014.10.044.
Prochazkova, L., Parkes, L., Dawson, A., Youssef, G., Ferreira, G.M., Lorenzetti, V., et al., 2017. Unpacking the role of self-reported compulsivity and impulsivity in obsessive-compulsive disorder. CNS Spectr. 21, 1–8. http://doi.org/10.1017/S1092852917000244.
Pruim, R.H.R., Mennes, M., Buitelaar, J.K., Beckmann, C.F., 2015a. Evaluation of ICA-AROMA and alternative strategies for motion artifact removal in resting state fMRI. Neuroimage 112, 278–287. http://doi.org/10.1016/j.neuroimage.2015.02.063.
Pruim, R.H.R., Mennes, M., van Rooij, D., Llera, A., Buitelaar, J.K., Beckmann, C.F., 2015b. ICA-AROMA: a robust ICA-based strategy for removing motion artifacts from fMRI data. Neuroimage 112, 267–277. http://doi.org/10.1016/j.neuroimage.2015.02.064.
Razi, A., Friston, K.J., 2016. The Connected Brain: causality, models, and intrinsic dynamics. IEEE Signal Process. Mag. 33 (3), 14–35. http://doi.org/10.1109/MSP.2015.2482121.
Razi, A., Kahan, J., Rees, G., Friston, K.J., 2015. Construct validation of a DCM for resting state fMRI. Neuroimage 106, 1–14. http://doi.org/10.1016/j.neuroimage.2014.11.027.
Razi, A., Seghier, M.L., Zhou, Y., McColgan, P., Zeidman, P., Park, H.-J., et al., 2017. Large-scale DCMs for Resting State fMRI, pp. 1–20. http://doi.org/10.1162/NETN_a_00015.
Reuter, J., Raedler, T., Rose, M., Hand, I., Gläscher, J., Büchel, C., 2005. Pathological gambling is linked to reduced activation of the mesolimbic reward system. Nat. Neurosci. 8 (2), 147–148. http://doi.org/10.1038/nn1378.
Robbins, T.W., Gillan, C.M., Smith, D.G., de Wit, S., Ersche, K.D., 2012. Neurocognitive endophenotypes of impulsivity and compulsivity: towards dimensional psychiatry. Trends Cogn. Sci. 16 (1), 81–91. http://doi.org/10.1016/j.tics.2011.11.009.
Satterthwaite, T.D., Elliott, M.A., Gerraty, R.T., Ruparel, K., Loughead, J., Calkins, M.E., et al., 2013. An improved framework for confound regression and filtering for control of motion artifact in the preprocessing of resting-state functional connectivity data. Neuroimage 64, 240–256. http://doi.org/10.1016/j.neuroimage.2012.08.052.
Satterthwaite, T.D., Wolf, D.H., Loughead, J., Ruparel, K., Elliott, M.A., Hakonarson, H., et al., 2012. Impact of in-scanner head motion on multiple measures of functional connectivity: relevance for studies of neurodevelopment in youth. Neuroimage 60 (1), 623–632. http://doi.org/10.1016/j.neuroimage.2011.12.063.
Stephan, K.E., Iglesias, S., Heinzle, J., Diaconescu, A.O., 2015. Translational perspectives for computational neuroimaging. Neuron 87 (4), 716–732. http://doi.org/10.1016/j.neuron.2015.07.008.
Stephan, K.E., Penny, W.D., Moran, R.J., den Ouden, H.E., Daunizeau, J., Friston, K.J., 2010. Ten simple rules for dynamic causal modeling. Neuroimage 49 (4), 3099–3109. http://doi.org/10.1016/j.neuroimage.2009.11.015.
Storch, E.A., Bagner, D., Merlo, L.J., Shapira, N.A., Geffken, G.R., Murphy, T.K., Goodman, W.K., 2007. Florida obsessive-compulsive inventory: development, reliability, and validity. J. Clin. Psychol. 63 (9), 851–859. http://doi.org/10.1002/jclp.20382.
Tavares, H., Gentil, V., 2007. Pathological gambling and obsessive-compulsive disorder: towards a spectrum of disorders of volition. Rev. Bras. Psiquiatr. 29 (2), 107–117. http://doi.org/10.1590/S1516-44462007000200005.
Tiego, J., Oostermeijer, S., Prochazkova, L., Parkes, L., Dawson, A., Youssef, G., et al., 2018. Overlapping dimensional phenotypes of impulsivity and compulsivity. CNS Spectr. 21, 1–15. http://doi.org/10.1017/S1092852918001244.
Tsvetanov, K.A., Henson, R.N.A., Tyler, L.K., Razi, A., Geerligs, L., Ham, T.E., et al., 2016. Extrinsic and intrinsic brain network connectivity maintains cognition across the lifespan despite accelerated decay of regional brain activation. J. Neurosci. 36 (11), 3115–3126. http://doi.org/10.1523/JNEUROSCI.2733-15.2016.
van Holst, R.J., van Holstein, M., van den Brink, W., Veltman, D.J., Goudriaan, A.E., 2012a. Response inhibition during cue reactivity in problem gamblers: an fMRI study. PLoS One 7 (3), e30909. http://doi.org/10.1371/journal.pone.0030909.
van Holst, R.J., Veltman, D.J., Büchel, C., van den Brink, W., Goudriaan, A.E., 2012b. Distorted expectancy coding in problem gambling: is the addictive in the anticipation? Bps 71 (8), 741–748. http://doi.org/10.1016/j.biopsych.2011.12.030.
van Timmeren, T., Daams, J.G., van Holst, R.J., Goudriaan, A.E., 2018. Compulsivity-related neurocognitive performance deficits in gambling disorder: a systematic review and meta-analysis. Neurosci. Biobehav. Rev. 84, 204–217. http://doi.org/10.1016/j.neubiorev.2017.11.022.
Verdejo-García, A., Lawrence, A.J., Clark, L., 2008. Impulsivity as a vulnerability marker for substance-use disorders: review of findings from high-risk research, problem gamblers and genetic association studies. Neurosci. Biobehav. Rev. 32 (4), 777–810. http://doi.org/10.1016/j.neubiorev.2007.11.003.
Whiteside, S.P., Lynam, D.R., 2001. The Five Factor Model and impulsivity: using a structural model of personality to understand impulsivity. Personal. Individ. Differ. 30 (4), 669–689. http://doi.org/10.1016/S0191-8869(00)00064-7.
Worhunsky, P.D., Malison, R.T., Rogers, R.D., Potenza, M.N., 2014. Altered neural correlates of reward and loss processing during simulated slot-machine fMRI in pathological gambling and cocaine dependence. Drug Alcohol Depend. 145, 77–86. http://doi.org/10.1016/j.drugalcdep.2014.09.013.
Yu, C.Y., 2002. Evaluating Cutoff Criteria of Model Fit Indices for Latent Variable Models with Binary and Continuous Outcomes. University of California Los Angeles.
Zhou, Y., Zeidman, P., Wu, S., Razi, A., Chen, C., Yang, L., et al., 2018. Altered intrinsic and extrinsic connectivity in schizophrenia. Ynicl 17, 704–716. http://doi.org/10.1016/j.nicl.2017.12.006.